

Interlayer tunnelling evidence for possible electron-boson interactions in $\text{Bi}_2\text{Sr}_2\text{CaCu}_2\text{O}_{8+\delta}$

T.M. Benseman* and J.R. Cooper

*Physics Department, Cavendish Laboratory, University of Cambridge,
J.J. Thomson Avenue, CB3 0HE, United Kingdom*

G. Balakrishnan

Department of Physics, University of Warwick, CV4 7AL, United Kingdom

(Dated: May 10, 2022)

We report intrinsic tunnelling data for mesa structures fabricated on three over- and optimally-doped $\text{Bi}_{2.15}\text{Sr}_{1.85}\text{CaCu}_2\text{O}_{8+\delta}$ crystals with transition temperatures of 86-80 K and 0.16-0.19 holes per CuO_2 unit, for a wide range of temperature (T) and applied magnetic field (H), primarily focusing on one over-doped crystal. The differential conductance above the gap edge shows clear structure with informative T and H dependence. Data below the gap edge imply that the tunnelling process is mainly coherent and give clear evidence for strong T -dependent pair breaking. These findings are important for a detailed analysis in terms of Eliashberg theory and could help to clarify the pairing mechanism.

Ever since the discovery of cuprate superconductors over 25 years ago, understanding the pairing mechanism has been an extremely active area of research. For classical strong-coupling superconductor such as Pb, precise measurement of the current-voltage ($I - V$) characteristics of planar tunnel junctions with a normal metal, or between two superconductors (SIS), shows good correlation between structure in dI/dV or d^2I/dV^2 above the superconducting (s/c) energy gap Δ , and the energy-dependent phonon density of states (DOS) measured by neutron scattering. Analysis using Eliashberg theory shows clearly that pairing is mediated by the virtual exchange of phonons [1]. The structure in dI/dV is caused by the energy (or frequency ω) dependence of two complex parameters: $\Delta(\omega)$, associated with s/c order and $z_s(\omega)$, arising from many-body, electron-phonon renormalization in the s/c state that are coupled via two integral equations. In the d -wave case they will also have strong momentum (\mathbf{k}) dependence.

Mesa structures fabricated from highly anisotropic high- T_c superconductors such as $\text{Bi}_2\text{Sr}_2\text{CaCu}_2\text{O}_{8+\delta}$ (Bi-2212) may be regarded as stacks of planar “intrinsic tunnel junctions” (ITJs) connected in series, and their $I - V$ characteristics correspond to c -axis, SIS tunnelling spectra [2]. Apart from a very recent paper [3], ITJs have not been used to detect structure in dI/dV that could give information about possible boson energies [4] and there are several reasons for this, see Footnote 5. However, tunnelling in planar ITJs may be easier to understand than in break junctions [6, 7] and being a bulk probe it could be a valuable complement to angle-resolved photoemission spectroscopy (ARPES) [8], optical reflectivity [4] and scanning tunnelling microscopy (STM) [9–11].

Here we report experimental data showing structure in the dI/dV curves of ITJs fabricated on two over-doped single crystals of Bi-2212 with T_c values of 80 and 78 K, OD80 and OD78, and an optimally doped crystal, OP86

with $T_c = 86$ K. We focus on OD80, for which there is clear structure above $2\Delta_0$, and where ARPES data gives evidence for a large Fermi surface and no pseudogap at low T [8]. Data for hole concentrations $p < 0.19$ per CuO_2 unit, may be complicated by the presence of the pseudogap and also of charge density waves that have been observed recently for both Bi-2212 [10, 11] and $\text{YBa}_2\text{Cu}_3\text{O}_{6.7}$ [12].

Single crystals of Bi-2212 were grown using a travelling solvent floating zone furnace and feed rods with nominal stoichiometry of $\text{Bi}_{2.15}\text{Sr}_{1.85}\text{CaCu}_2\text{O}_{8+\delta}$. These have a maximum T_c of 86.5 K and we infer p from the empirical relation $T_c = T_c^{\text{max}}(1 - 82.6[p - 0.16]^2)$ [13], finding $p = 0.194, 0.191$ and 0.16 for the three crystals studied. For OD78 and OD80, T_c measured by Squid magnetometry before fabrication of mesas agreed with values deduced from mesa dI/dV curves, e.g. Fig. 2(b), to within 1 K but for OP86, T_c from dI/dV curves could be up to 3 K lower than the magnetometry data. Typical $I - V$ characteristics for the three mesas at small bias, measured when increasing I , are given as supplemental material (SM). The branches in the $I - V$ characteristic correspond to different numbers of Josephson junctions being switched into the resistive state. The number of junctions (N) in the stack is equal to the total number of branches observed. In the SM it is shown that these branches scale on to each other, confirming that the junctions in the mesa have uniform area, and therefore all junctions switched to the resistive state will have the same voltage bias.

Mesa dI/dV spectra [14] were measured as the bias current was swept down from its maximum value towards zero, thereby maintaining the resistive state. A lock-in technique with a small 77.7 Hz current modulation was employed. Fig. 1(a) shows dI/dV per unit area for a single junction of OD80, at 1.4 K *vs.* the bias voltage per junction, for $H = 0$ to 13T applied perpendicular to the CuO_2 planes. The curves are symmetric for $\pm V$, so for

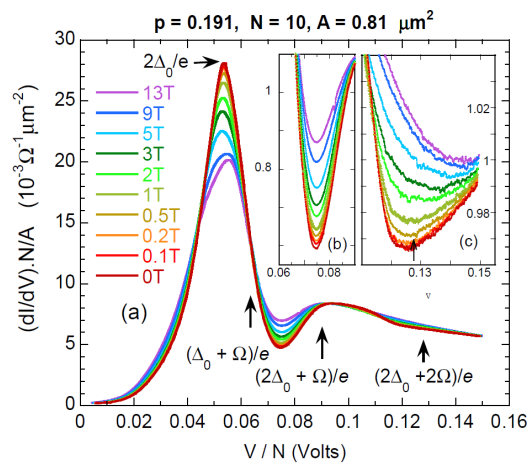


FIG. 1: Color online: (a) dI/dV curves for OD80 at 1.4 K in various magnetic fields applied perpendicular to the CuO_2 planes plotted *vs.* V/N , the bias voltage per junction. (b) and (c) show details of the field dependence of the lower and upper dips. Here dI/dV curves have been normalized by dividing through by the polynomial given in the text. Values of $(\Delta_0 + \Omega)/e$, $(2\Delta_0 + \Omega)/e$ and $2(\Delta_0 + \Omega)/e$ are shown by arrows (see text).

clarity we only show data for $V > 0$. For such SIS junctions the sharp peaks are located at voltages of $2\Delta_0/e$, where Δ_0 is the maximum value of the d -wave gap. At 1.4 K this gives $\Delta_0 = 27.3$, 26.9 and 27.4 meV for OD78, OD80 and OP86 respectively, in good agreement with the lower values shown in Fig. 15 of Ref. 9 for these doping levels. The ratio $2\Delta_0/k_B T_c = 8.08 \pm 0.1$, 7.83 ± 0.1 and 7.5 ± 0.15 for these three mesas is ~ 1.75 - 1.9 times larger than for a weak-coupling d -wave superconductor.

In order to see whether tunnelling is coherent, i.e. whether it conserves \mathbf{k} parallel to the CuO_2 planes, we make a log-log plot of $dI/dV - (dI/dV)_{res}$ *vs.* V , where $(dI/dV)_{res}$ is the extrapolated value at $V = 0$. As shown in the SM, for all three mesas this gives a limiting V^4 law for $V < 0.74\Delta_0$, whereas a V^2 law is expected for completely incoherent tunnelling. It should be possible to account for this V^4 law by including both the angle-dependence of the c -axis transfer integral, which goes to zero in the nodal directions [15], and the Dynes damping factor [16], i.e. the imaginary part of $\Delta(\omega)$. As mentioned already, this is likely to be much more ω and \mathbf{k} dependent than in the s -wave case. Defects in the barrier regions could scatter the tunnelling electrons sufficiently to give limited incoherence, i.e. a spread in \mathbf{k} values [17] and this would be most significant in the nodal regions.

The data for OD80 in Figs. 1(a)-(c), show two field (H) dependent dips above $eV = 2\Delta_0$. For clarity of display, the data in Figs. 1(b) and (c) have been normalized by dividing through by the polynomial $(8.85 - 151.27V^2 + 501.22V^4) \times 10^{-3}\Omega^{-1}\mu m^{-2}$, where V is the voltage per

junction, see Footnote 18.

For coherent tunnelling, the angle θ between \mathbf{k} and the anti-nodal direction is conserved. Within the standard “semiconductor” model [1], for a d -wave energy gap varying as $\Delta_0 \cos(2\theta)$ and a single \mathbf{k} -independent boson energy Ω , boson-induced structure is expected to be most apparent at $eV = 2\Delta_0 + \Omega$. At this bias voltage, the gap edge at Δ_0 for $\theta = 0$ on one side of the junction has the same energy as any structure at $\Delta_0 + \Omega$ and $\theta = 0$ on the other side. The effect is larger there because the peak in the s/c quasi-particle DOS is largest at $\theta = 0$, with further enhancement from the larger normal state DOS [19] and tunnelling matrix elements [15]. Additional structure is expected near $eV = 2\Delta_0 + 2\Omega$ where boson-induced anomalies on each side of the junction at $\theta = 0$ have the same energy. The $S=1$, magnetic resonance excitation, seen by inelastic neutron scattering [20], is a candidate pairing boson [19, 21]. It has an energy $\Omega = 5.4k_B T_c$ [19, 20] and a momentum vector \mathbf{Q} , close to $(\pi/a, \pi/a)$, [19, 20] where a is the in-plane lattice spacing. Various energies associated with this value of Ω are shown in Fig. 1 and later for all three mesas in Fig. 3. It can be seen that there is only rough correspondence with the simple description given above. There is also strong H and T -dependence as amplified below.

The quasi-particle DOS produced by a magnetic field in a d -wave superconductor, is predicted [22] to be $\sim N(0)(H/H_{c2})^{1/2}$, where H_{c2} is the upper critical field and $N(0)$ is the electronic DOS at the Fermi energy in the normal state. This pair breaking effect arises from Doppler shifts in the energies of $+\mathbf{k}$ and $-\mathbf{k}$ states caused by the superfluid flow in the vortex state. For low H , pairs are broken near the nodes, where the s/c gap is small, but the region widens as H is increased. The effect is seen in heat capacity studies of $YBa_2Cu_3O_7$ crystals, for example Ref. 23. As shown in Fig. 1(a), the low bias data show very little H -dependence. This is presumably because of the strong θ dependence for coherent c -axis tunnelling as explained in Refs. 15, 19. In contrast, the lower dip is strongly suppressed by fields of 13T applied perpendicular to the CuO_2 planes and as shown later in Fig. 4(a), for OD80 it varies as $A + BH^{1/2}$, where A and B are fitting parameters. This must mean that the lower dip is strongly affected by the presence of pairs in the nodal regions. When they are broken by the applied field then the lower dip is attenuated. In contrast, as shown in Fig. 4(b), dI/dV at low V varies approximately as $A + BH^1$. The H -dependence of the upper dip is assessed by plotting dI/dV at 125 mV *vs.* H in Fig. 4(c). Here the two OD mesas show remarkably similar behavior while the effect for OP86 is a factor of two larger. Differences between the two OD mesas at lower V in Figs. 4(a) and (b) are probably caused by the sensitivity of the nodes to inter- and intra-layer scattering processes.

Fig. 2(a) shows the overall T -dependence of our raw dI/dV data for OD80 in zero field at selected tempera-

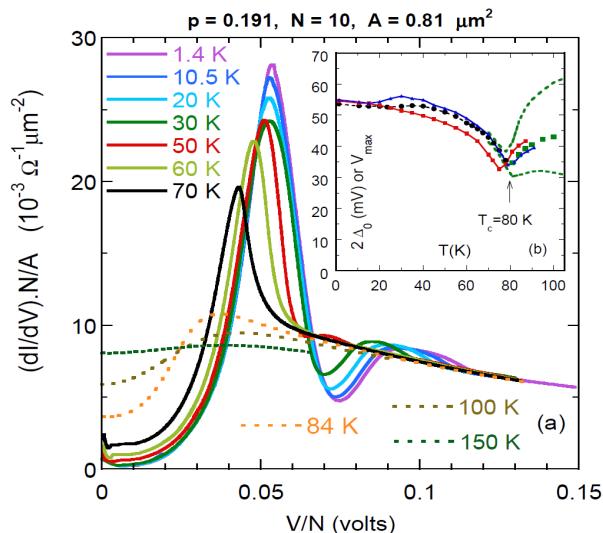


FIG. 2: Color online: (a) dI/dV curves for OD80 at selected values of T , see the SM for the complete data set. (b) T -dependence of the d -wave gap $2\Delta_0(T)$ up to T_c from the main peaks in dI/dV for OD80 (black circles), OD78 (red squares) and OP86 (blue triangles). For OD80, green squares above $T_c=80$ K give voltages of broad maxima in dI/dV . Green dashed lines show their increased breadth by marking regions where $dI/dV \geq 0.95(dI/dV)_{MAX}$.

tures. The data in Fig. 2(a) and for all three mesas in Fig. 3 show that the dip and the hump at higher V , are strongly T -dependent and have almost disappeared at 50 K even though Δ_0 has hardly changed from its low T value there. The attenuation of the hump is much smaller up to 40 K, but it shifts up with increasing T and also disappears rapidly between 50 and 60 K. It seems that this strong T -dependence, especially the shifts of the dips and humps with T , is unlikely to be caused by a conventional phonon pairing mechanism. As shown in Fig. 3, the lower dip is partially suppressed by a magnetic field, but it is not shifted, unlike the effect of temperature. For all three mesas a relatively sharp fall in $2\Delta_0(T)$ also sets in just above 50 K as shown in Fig. 2(b). A striking feature of Fig. 2(b) is that just below T_c , $2\Delta_0(T) \simeq \Omega = 5.4k_B T_c$, possibly suggesting that the integrity of the magnetic mode is essential for superconductivity [19].

The dI/dV curves in Fig. 2(a) above T_c also have peaks whose breadth increases rapidly with T as indicated by the green dashed lines for OD80 in Fig. 2(b). They appear to be states-conserving, for example at 84 K the polynomial normalization used earlier gives a dI/dV curve that conserves states to within 2.2% for the range of V shown in Fig. 2(a). The presence of these broad peaks for $p = 0.19$ agrees with the recent laser ARPES study of Bi-2212 showing a trisected s/c dome [8] and a pseudogap above T_c extending up to $p = 0.22$. But at low T the pseudogap sets in abruptly below $p = 0.19$ [8] in agreement with earlier heat capacity [24] and penetra-

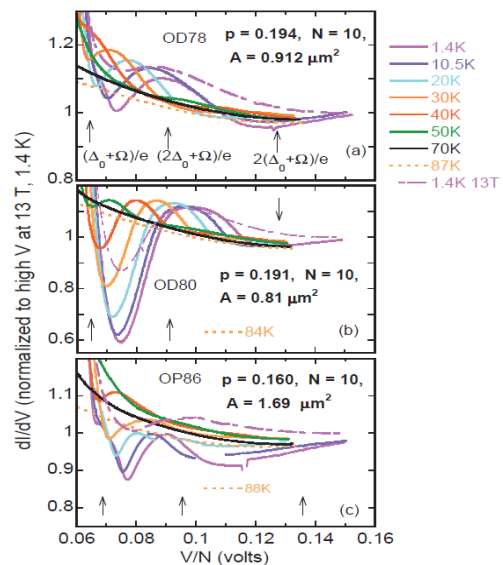


FIG. 3: Color online: Zoom of the structure above the gap edge, for (a) OD78, (b) OD80 and (c) OP86 at selected T . The data have been normalized for clarity, see Footnote 18. Full data sets including un-normalized data are given in the SM. Data at 1.4 K for a magnetic field of 13 T $\parallel c$ are also shown.

tion depth [25] measurements. We note that the energies of the broad peaks above T_c are comparable with $2\Delta_0$, so if they are caused by a competing mechanism [8] this would also tend suppress superconductivity once $2\Delta_0(T)$ falls below a certain value.

As recognized previously [9], the T -dependence of the data in Fig. 2(a) at low bias cannot be ascribed simply to thermal broadening. This is shown explicitly in Fig. 4(d) where the effect of thermal broadening has been calculated by smoothing the dI/dV vs. V data at 1.4 K over a voltage window of $4k_B T/e$. We therefore conclude that the larger values of dI/dV at low V , i.e. $(dI/dV)_{res}$ are caused by T -dependent pair-breaking processes in line with early junction work [7]. The magnitude of the scattering rate $(1/\tau_{pb})$ estimated from the energy broadening of the curves at low bias in Fig. 4(d) is surprisingly large, $\hbar/\tau_{pb} \simeq 14.5$ meV or 170 K at 50 K. If real electron-boson scattering processes are responsible for $1/\tau_{pb}$ then its T -dependence will be related to the boson DOS. In Fig. 4(e) we plot $(dI/dV)_{res}$ vs. T . Normalized data for the three mesas are in excellent agreement, the data for OD78 and OD80 obey an $A + BT^4$ law, while for OP86, $A + BT^3$ gives a marginally better fit. Finally in Fig. 4(f) we show that the amplitude of the dip-hump feature for OD80 obeys an $A - BT^2$ law to high accuracy. The amplitude for OD78 is smaller and is not such a good fit to $A - BT^2$, probably because of non-ideal behavior near the nodes.

In summary we have reported intrinsic SIS planar tunnelling data for three crystals of the cuprate superconduc-

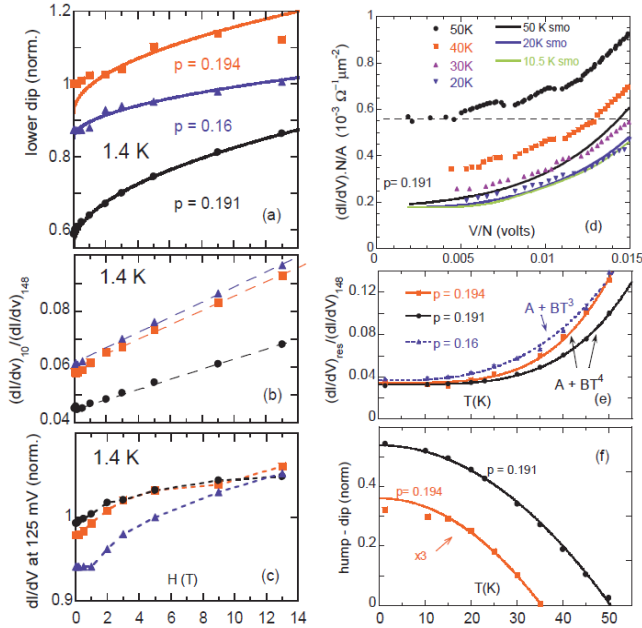


FIG. 4: Color online: (a) normalized minima near 75 mV (lower dips) *vs.* H for the three mesas at 1.4 K, solid lines show fits to $A + BH^{1/2}$, where A and B are fitting parameters. (b) dI/dV at low bias (10 mV) normalized to high bias (148 mV) *vs.* H . (c) dI/dV at a fixed voltage near upper dip (125 mV) *vs.* H , dashed lines are guides to the eye. (d) Zoom of some of the data for OD80 at low bias. Solid symbols show measured values, lines show the 1.4 K data smoothed by $4k_B T$ to see the effect of thermal broadening. The horizontal dashed line shows that at 50 K the energy broadening is 14.5 meV. (e) T dependence of the residual value of dI/dV at low V , which is caused by pair breaking, normalized to dI/dV at 148 mV for the three mesas. Fits to $A + BT^4$ (solid lines) and $A + BT^3$ (dashed line) are also shown. (f) T -dependence of the maximum in dI/dV at the “hump” minus the minimum at the “dip”, for OD80 and OD78, showing $A - BT^2$ behavior, data for OP86 are less smooth and are not shown.

tor Bi-2212, and discussed their field- and temperature-dependence. We argue that the dip structure must be connected with the nodes, presumably via the Eliashberg equations, because it is destroyed by H or T -induced pair-breaking. Accounting for this fact in terms of the magnetic mode that has $\mathbf{Q} \simeq (\pi/a, \pi/a)$ [19, 20] will be a strong test of this pairing model. T -dependent inelastic scattering is strong in the nodal regions, and could possibly be caused by the same excitations whose virtual exchange is providing the pairing “glue”.

We would like to thank V. Krasnov and J.L. Tallon for helpful discussions and advice, E.J. Tarte and M. Weigand for assistance with lithographic mask design, staff at the Cambridge Nanosciences Centre for their help over a long period and A. Carrington for comments on the manuscript.

* Present address: Materials Science Division, Argonne National Laboratory, Argonne, IL 60439.

- [1] E.L. Wolf, “Principles of Electron Tunnelling Spectroscopy”, Oxford University Press, New York, (1989) Chapter 4.
- [2] A.A. Yurgens, Supercond. Sci. Technol. **13**, R85-R100 (2000).
- [3] X-H. Sui, H. Tang, S.P. Zhao, Z-B. Su, Physica C (2015), doi:http://dx.doi.org/10.1016/j.physc.2015.02.005.
- [4] J.P. Carbotte, T. Timusk and J. Hwang, Rep. Prog. Phys. **74**, 066501 (2011).
- [5] (a) The power dissipation per unit area in HTS mesa structures is large, sometimes resulting in extreme distortion of $I - V$ curves by self-heating effects and consequent obliteration of any weak features in dI/dV . Zhu *et al.* [26] have studied mesa structures in near-optimally doped Bi-2212 containing $N = 10 - 11$ junctions in series, finding that there is little heating-induced distortion of the $I - V$ characteristic only when the mesa area A is $\simeq 1 \mu\text{m}^2$ or less. Our mesas have $N \cdot A$ below this limit and a dozen or so junctions or less. (b) A high level of oxygen homogeneity in the mesa is necessary to ensure that any resonances are clearly observed. To avoid possible problems with ion milling [27], we fabricate our mesas solely by chemical wet etching [14]. (c) irrespective of the size of the mesas, there is a possibility of electron heating. For a given V this will not depend on N or A but only on the electrical resistance of the junction per unit area and the thermal resistance for heat transfer between quasi-particles and phonons. We can rule this out for the three mesas in Fig. 3 because their structure at higher V continues to evolve between 10 and 1.4 K.
- [6] O. Ahmadi, L. Coffey, J. F. Zasadzinski, N. Miyakawa and L. Ozyuzer, Phys. Rev. Lett. **106**, 167005 (2011).
- [7] D. Mandrus, L. Forró, D. Koller and L. Mihály, Nature **351**, 460 (1991).
- [8] I. M. Vishik, M. Hashimoto, R-H. He, W-S Lee, F. Schmitt, D. Lu, R. G. Moore, C. Zhang, W. Meevasana, T. Sasagawa, S. Uchida, K. Fujita, S. Ishida, M. Ishikado, Y. Yoshida, H.I. Eisaki, Z. Hussain, T. P. Devereaux and Z-X Shen, Proc. Nat. Acad. Sci. **109**, 18331 (2012).
- [9] Ø. Fischer, M. Kugler, I. Maggio-Aprile, C. Berthod and C. Renner, Rev. Mod. Phys. **79**, 353-419 (2007).
- [10] K. Fujita, C. K. Kim, I. Lee, J. Lee, M. H. Hamidian, A. Firmo, S. Mukhopadhyay, H. Eisaki, S. Uchida, M. J. Lawler, E.-A. Kim and J. C. Davis, Science, **344**, 612 2014.
- [11] E.H. da Silva Neto, P. Aynajian, A. Frano, R. Comin, E. Schierle, E. Weschke, A. Gyenis, J. Wen, J. Schneeloch, Z. Xu, S. Ono, G. Gu, M. Le Tacon and A. Yazdani, Science, **343**, 393 (2014).
- [12] J. Chang, E. Blackburn, A. T. Holmes, N. B. Christensen, J. Larsen, J. Mesot, R. Liang, D. A. Bonn, W. N. Hardy, A. Watenphul, M. v. Zimmermann, E. M. Forgan, and S. M. Hayden, Nat. Phys. **8**, 871 (2012).
- [13] M. R. Presland, J. L. Tallon, R. G. Buckley, R. S. Liu and N. E. Flower, Physica C **176**, 95 (1991).
- [14] T.M. Benseman, Ph.D thesis, University of Cambridge, March, 2007.
- [15] O. K. Andersen, A. I. Liechtenstein, O. Jepsen and E Paulsen, J. Phys. Chem. Solids **56**, 1573-1591 (1995).

- [16] R. C. Dynes, V. Narayanamurti, and J. P. Garno, Phys. Rev. Lett. **41**, 1509 (1978).
- [17] J. R. Cooper, Phys. Rev. B **76**, 064509 (2007).
- [18] The three polynomials for the three mesas were found by requiring the normalized dI/dV curves for $H=13$ T and 1.4 K, to be unity at high V , 0.142-0.15 V, with zero slope and to conserve states from 0-0.15 V.
- [19] M. Eschrig, Advances in Physics **55**, 47-183 (2006).
- [20] H. He, Y. Sidis, P. Bourges, G. D. Gu, A. Ivanov, N. Koshizuka, B. Liang, C. T. Lin, L. P. Regnault, E. Schoenherr, and B. Keimer, Phys. Rev. Lett. **86**, 1610 (2001).
- [21] D.J. Scalapino, Rev. Mod. Phys. **84**,1383-1417 (2012).
- [22] G. E. Volovik, JETP Lett. **58**, 469 (1993).
- [23] Y. Wang, B. Revaz, A. Erb and A. Junod, Phys. Rev. B **63**, 094508 (2001).
- [24] J. W. Loram, J. Luo, J. R. Cooper, W. Y. Liang and J. L. Tallon, J. Phys. Chem. Solids **62**, 59 (2001).
- [25] W. Anukool, S. Barakat, C. Panagopoulos and J. R. Cooper, Phys. Rev. B **80**, 024516 (2009).
- [26] X. B. Zhu, Y. F. Wei, S. P. Zhao, G. H. Chen, H. F. Yang, A. Z. Jin and C. Z. Gu, Phys. Rev. B **73**, 224501 (2006).
- [27] V. M. Krasnov, A. Yurgens, D. Winkler, P. Delsing and T. Claeson, Phys. Rev. Lett. **84**, 5860 (2000).

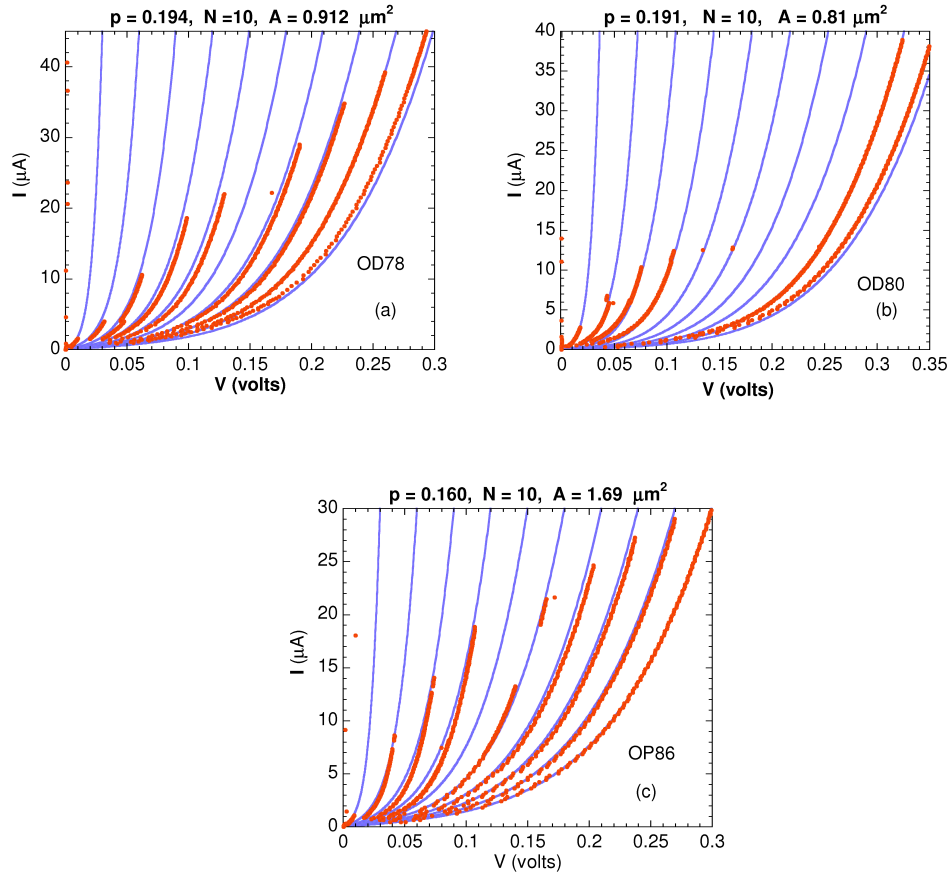


FIG. 5: Supplemental Material. Typical $I - V$ curves for the three mesas taken while sweeping the current up and down in a controlled manner, red points show data, blue lines are fits. Switching to another branch occurs when the critical (Josephson) current of a particular junction is exceeded and a voltage develops across it. The current is then swept down to a finite value before being increased again. Eventually, all Josephson currents are suppressed and the extreme right hand red curves, with the largest values of V are obtained. These are the same curves as those measured on downward sweeps, typically from $V = 1.5$ V to 0.05 V, and for which dI/dV is measured using a lock-in technique. The blue lines show fits of the form $I = aV + bV^3 + cV^5$ to the $(N-1)$ th curve which are then scaled by $n/(N-1)$ where n is an integer between 1 and N , for comparison with the measured values shown by red points. Differences between the red data points and the blue lines give an indication of possible non-uniformity in junction areas.

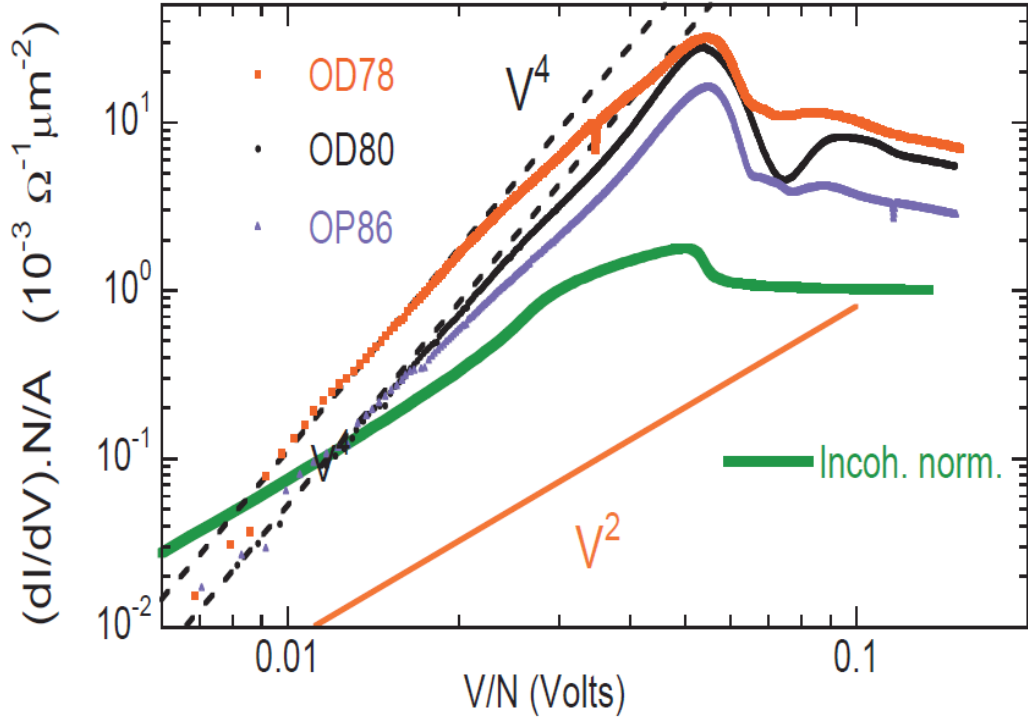


FIG. 6: Supplemental Material. This Figure provides confirmation of the statements at the bottom of the first column of page 2 of our paper. The log-log plots show that the dI/dV data at 1.4 K and 0 T for all three mesas obey the law $A + BV^4$, below 20 mV or $0.74\Delta_0$. In the above figure the residual values A which have been subtracted are 0.309, 0.203 and $0.117 \times 10^{-3} \Omega^{-1} \mu\text{m}^{-2}$ for OD78, OD80 and OP86 respectively. The calculated curve for completely incoherent tunnelling (no \mathbf{k} conservation) between two weak-coupling d -wave superconductors is also shown. It has a completely different shape and a limiting V^2 dependence below $V/N = 0.7 \Delta_0$.

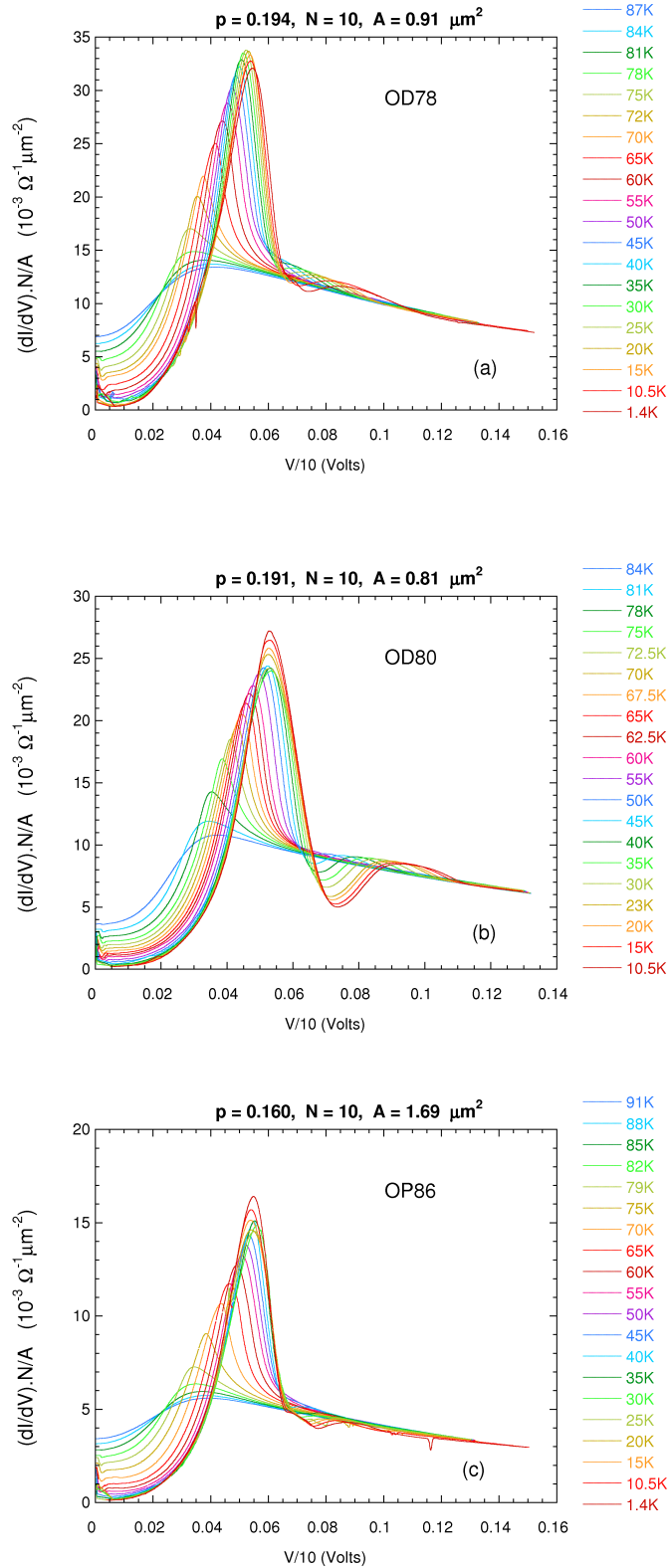


FIG. 7: Supplemental Material. This Figure shows T -dependent tunnelling data for all three mesas at all values of T (the data for OD80 at 1.4 K are shown in Fig.2 of the paper). The areas of the mesas were measured by scanning electron microscopy.

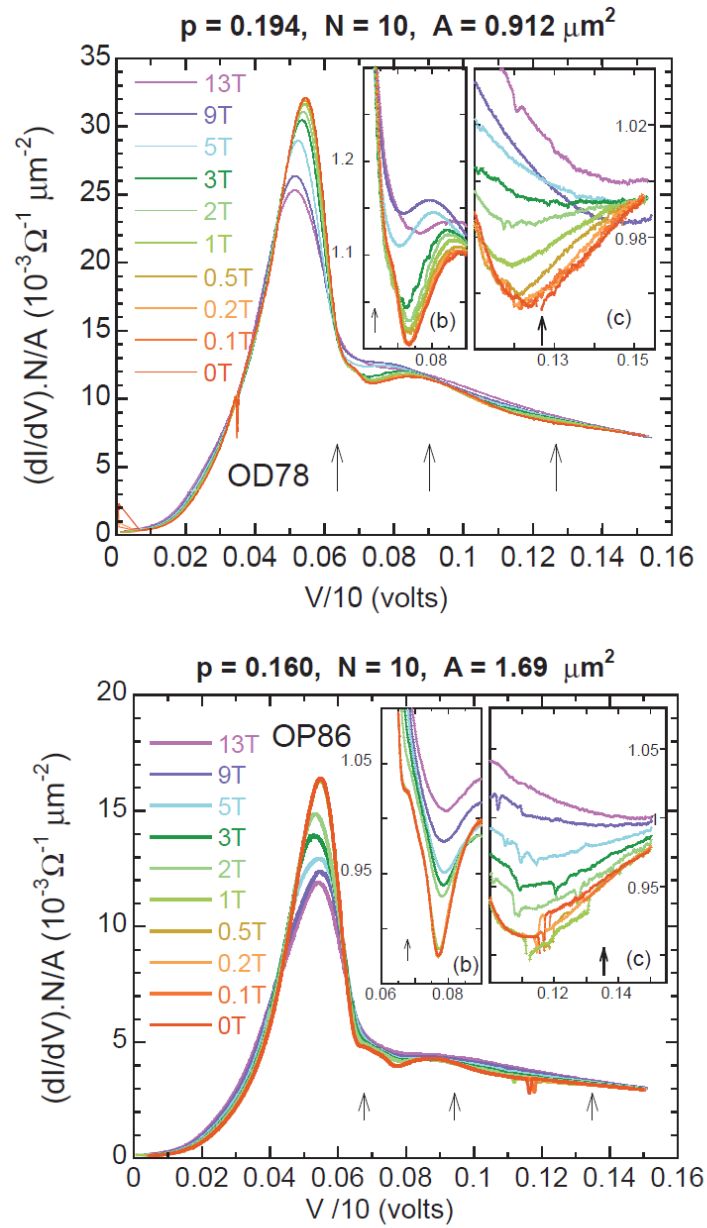


FIG. 8: Supplemental Material. This Figure shows the tunnelling data at 1.4 K in fields from 0 to 13 T applied perpendicular to the CuO_2 planes, for mesas OD78 and OP86 together with zooms of the lower and upper dips. The equivalent data for mesa OD80 are shown in Figure 1 of the paper.

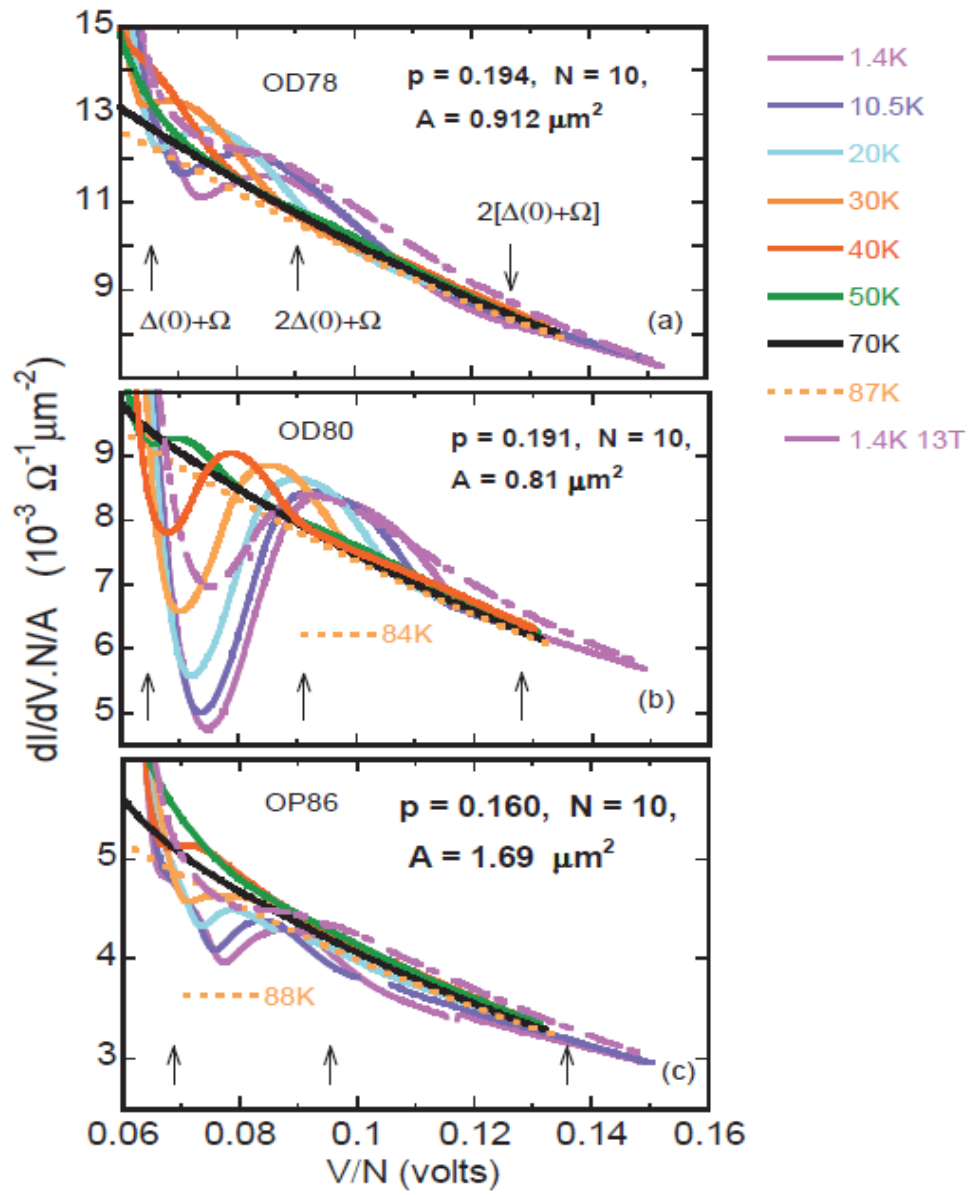


FIG. 9: Supplemental Material. This figure shows the same data as in Fig. 3 of the paper but without normalization.